Science of the Total Environment xxx (xxxx) 169045

Contents lists available at ScienceDirect

Science of the Total Environment

journal homepage: www.elsevier.com

Serpentinization-associated travertines as spatio-temporal archives for lipid biomarkers key for the search for life on Mars

Laura Sánchez-García [a,*], Daniel Carrizo [a], Pablo Jiménez-Gavilán [b], Lucía Ojeda [b], Víctor Parro [a], Iñaki Vadillo [b]

[a] Centro de Astrobiología (CAB, CSIC-INTA), 28850 - Torrejón de Ardoz, Madrid, Spain
[b] Department of Geology, Faculty of Science, University of Malaga, 29071 Malaga, Spain

ARTICLE INFO

Editor: Christian Herrera

Keywords:
Lipid biomarkers
Preservation
Biogenicity
Serpentinization
Mars

ABSTRACT

Serpentinization is a well-known aqueous alteration process that may have played important roles in the origins and early evolution of life on Earth, and perhaps Mars, but there are still aspects related to biomarker distribution, partitioning, and preservation that merit further study. To assess the role that precipitation of carbonate phases in serpentinization settings may have on biomarker preservation, we search for life signs in one of the world's largest outcrops of subcontinental peridotites (Ronda, South Spain). We investigate the organic record of groundwater and associated carbonate deposits (travertines) in seven hyperalkaline springs, and reconstruct the biological activity and metabolic interactions of the serpentinization-hosted ecosystem. We identified lipid biomarkers and isotopic evidences of life, whose concentration and variety were much lower in groundwater than travertine deposits (ppb/ppt versus ppm level). Groundwater carried organics of abiotic (*n*-alkanes with values of CPI ~ 1) and/or biotic origin, of fresher (e.g. acids or alcohols) or more diagenetized (mature hopanes and *n*-alkanes) nature. In contrast, associated travertines held a more prolific record of biomarkers incorporating (molecular and isotopic) fingerprints of surface (mostly phototrophs) and subsurface (chemolithotrophs, methanogens and/or methanotrophs) life. Serpentinization-associated travertines seem to act as biomolecule archives over time fed by autochthonous and allochthonous sources, hence amplifying the dim biological signal of groundwater. These results illustrate the relevance of serpentinization-associated surface mineral deposits in searching for traces of life on analogous environments on Mars. We highlight the diversity of lipids produced in serpentinizing land environments and emphasize the potential of these geostable biomolecules to preserve fingerprints of life.

1. Introduction

Serpentinizing systems are intriguing environments with interest for understanding the origin of life on Earth and its implications for astrobiology (Martin et al., 2008; Schulte et al., 2006). They are unique settings where the aqueous alteration of low-silica ultramafic rocks liberates carbon, energy and reducing power (Russell et al., 2010). It also provides raw materials critical to the synthesis of new biomass and the functioning of cells (e.g., phosphorus and boron) (Schrenk et al., 2013). Serpentinization is a process globally distributed on Earth in oceanic crusts and locations where tectonic processes lead to the uplift and exposure of mantle materials (Martin et al., 2008). It is the exothermic hydration, carbonation and oxidation of ultramafic rocks whereby serpentinite is produced from the alteration of olivine and pyroxene comprising this ocean crust, and much of the ferrous iron within the fayalite (Fe_2SiO_4) portion of olivine is oxidized to magnetite (Fe_3O_4). Concomitantly, some water is reduced to hydrogen, the carbon dioxide is then hydrogenated to methane (Proskurowski et al., 2008), and highly alkaline fluids are produced (Schrenk et al., 2013). Furthermore, serpentinization may also be behind the generation of magnetic carriers in the early Martian crust (Quesnel et al., 2009; Yu and Ni, 2023) of generally mafic composition (Hurowitz et al., 2023). Notably, the Séítah formation in the floor of Jezero Crater is composed of olivine-rich and carbonate-bearing rocks, as multispectral images and x-ray fluorescence data acquired by the Perseverance rover have recently confirmed (Liu et al., 2022). Further, evidences of past serpentinization have been reported on the surface of other planetary bodies in the Solar System, such as Ceres (Milliken and Rivkin, 2009), and it is considered likely to

* Corresponding author.
E-mail address: lsanchez@cab.inta-csic.es (L. Sánchez-García).

https://doi.org/10.1016/j.scitotenv.2023.169045
Received 29 September 2023; Received in revised form 28 November 2023; Accepted 30 November 2023
0048-9697/© 20XX

drive the hydrothermal energy circulation in Europa's subsurface ocean (Vance et al., 2007).

Serpentinization provides energy and raw materials that support chemosynthetic microbial communities in the deep subsurface and thus, it emerges as an attractive venue for the origin of life. First, serpentinization systems host highly reducing conditions rich in H_2, a crucial component for the prebiotic synthesis of organics and every biochemical reduction or oxidation reaction in modern metabolic pathways (Nealson et al., 2005). Indeed, one of the earliest metabolic pathways (i.e. the reductive acetyl-CoA or Wood-Ljungdahl pathway) is largely driven by H_2 (Cody and Scott, 2007). Second, serpentinite-hosted environments feature characteristic gradients of temperature, pH, redox, geochemistry, or porosity, all promoting prebiotic scenarios and favoring early evolution (Schrenk et al., 2013). Third, phosphate (i.e. a macro-nutrient essential to microbial communities and a fundamental component of nucleic acids and bacterial membrane lipids; Bradley et al., 2009) can be available in serpentinizing environments, accumulating in the phosphate-containing mineral hydroxyapatite and brucite (Schrenk et al., 2013), an effective scavenger of both phosphorous and boron, another key element that may have supported RNA synthesis (Holm et al., 2006). Overall, the theories of the RNA world are compatible with thermodynamically favorable H_2-rich settings (e.g. serpentinization active sites). Finally, carbonate veins produced by serpentinization may also serve as a shelter to preserve biomarkers over geological timescales (Klein et al., 2015; Newman et al., 2020). Thus, if life ever occurred on Mars, it is likely to have arisen in an environment such as those generated by serpentinization.

On Mars, the finding of serpentine outcrops and alteration minerals throughout the southern highland suggests that serpentinization could have been a common and widespread process in the Noachian (Quesnel et al., 2009; Ehlmann et al., 2010), a period when conditions of warmer and wetter climate could have supported microbial life (Ehlmann et al., 2011). Searching for signs of life corresponding to such ancient periods (4.1–3.7 Gyr), the most likely for a possible Martian life, requires a remarkable capacity to preserve putative biomarkers. Lipids are geostable biomolecules with applicability and potential to meet this requirement better than others, such as nucleic acids or proteins (Sánchez-García et al., 2021). They are the earliest reported molecular evidences of life (1.73 Ga old) on Earth (Vinnichenko et al., 2020), and their long-term preservation is largely documented in the sedimentary rock record (Sánchez-García et al., 2021; Brocks and Schaeffer, 2008; Saito et al., 2017; Birgel and Himmler, 2008). The ability to persist over time as biomarkers depends not only on the structural quality of the biomolecules but also, to a large extent, on the physico-chemical conditions of the deposition environment, either promoting or preventing their degradation. On Mars, the highly-oxidizing conditions derived from the exposure to ionizing radiation and the prevalence in the regolith of perchlorates (Hays et al., 2017) reduce the chances of finding any molecular fossil of life on the surface to virtually zero. Alternatively, the Martian subsurface emerges as an interesting target to search for possible life remnants as it provides mineral protection and rocky shielding (Hays et al., 2017). Notably, serpentinite-hosted environments are below the zone affected by solar and cosmic radiation and provide reducing conditions at a few millimeters from the high-energy surface. Therefore, serpentinization provides not only a propitious scenario for the emergence of life, but also suitable conditions for preserving its remnants.

Wherever serpentinization occurs, it may support microbial (chemolithoautotrophic) life (Schrenk et al., 2013 and references therein). Yet, aspects related to geosphere-biosphere interactions, as well as the distribution, partitioning, and preservation of putative biomarkers are insufficiently understood. In particular, terrestrial serpentinization systems are poorly studied compared to active oceanic sites (e.g. Suzuki et al., 2013), and their lipidome remains scarcely characterized. Here, we investigate the occurrence of lipid biomarkers in serpentinizing-hosted environments from one of the largest outcrops (~450 km²) of subcontinental mantle peridotite worldwide: the Ronda peridotite massifs (Fig. 1). We report molecular and isotopic fingerprints of life in groundwater and associated travertine deposits of seven hyperalkaline springs, including biomarkers of methanotrophic and/or methanogenic activity. Travertine deposits precipitate at the surface by interaction of Ca-OH type groundwater, and Mg-HCO_3 type waters from subsurface or relatively shallow flows and rivers (Giampouras et al., 2019). The travertines accumulate biomarkers over time from both the subsurface and surface, allochthonous and autochthonous sources, and prokaryotic and eukaryotic life. They act as integrative time and spatial records of biomarkers from serpentinization-associated life, thus arising as a key target in the search for past life on Mars, where a putative life related to serpentinization in early Martian epochs could have left its traces in associated carbonate deposits.

2. Materials and methods

2.1. Serpentinization in the Ronda peridotite massifs

In the westernmost part of the Málaga province (South Spain), the Ronda peridotite massifs constitute one of the worldwide most extensive outcrops of subcontinental mantle ultramafic rocks, whose geology has been extensively studied (e.g. Acosta-Vigil et al., 2014; Gervilla et al., 2002). Major fracturing in the central part of the massif favors fluid circulation that leads to intense hydrothermal alteration of the rocks, with an important degree of superficial serpentinization as a result of the atmospheric transformation of olivine (superficial hydration) (Obata, 1980). The high fracturing, weathering and superficial serpentinization process allow the development of a more or less important alteration layer that drains groundwater that emerges in subsurface springs, the so-called epiperidotitic springs (Jiménez-Gavilán et al., 2021) and hyperalkaline springs (Vadillo et al., 2015; Etiope et al., 2016). In the hyperalkaline springs, groundwater is deep and flows long distances (water ages dating from ≥2 ky; Etiope et al., 2016) in favor of major or minor mechanical contacts (thrust and inverse faults). These hyperalkaline waters show higher temperatures than average air temperature and hyperalkaline pH values (up to 12) due to the chemical interactions with deep-seated ultramafic rocks (Giampouras et al., 2019). Upon emergence, the Ca-OH-rich groundwater gets in contact with surface O_2 and CO_2 and mixes with Mg-HCO_3-rich water from both epiperidotitic flows and rivers/streams, which induces the formation of travertines (Giampouras et al., 2019).

In Ronda, the hyperalkaline springs are rich in CH_4 (0.1 to 3.2 mg·l^{-1}) and vent the gas to the atmosphere through active bubbling and diffuse seepages (Etiope et al., 2016). Most of the CH_4 is of abiotic origin according to its stable-carbon isotopic composition ($\delta^{13}C_{CH4}$ of −12.3 to −37 ‰), their molecular gas composition (presence of ethane and propane), the absence of radiocarbon (^{14}C) in CH_4 and the clumped isotope thermodynamic disequilibrium (Etiope et al., 2016; Ojeda et al., 2023). However, in some springs (e.g. FA and BFA), CH_4 seems to rather stem from mixed biotic-abiotic sources ($\delta^{13}C_{CH4}$ of −54 to −69 ‰) (Etiope et al., 2016). In addition, the released CH_4 is considered to be mostly allochthonous (i.e. not generated from the carbon in the hyperalkaline water), according to the fossil ^{14}C ages measured for CH_4 (> ca. 50,000 y BP) in comparison to that of dissolved inorganic carbon in the springs (from modern to 2334 y BP) (Etiope et al., 2016).

2.2. Sampling description

In March 2022, a field campaign was conducted to collect samples from seven serpentinization-hosted hyperalkaline springs from the Ronda peridotite massifs (Fig. 1): Baños del Duque (BD), Fuente Romana (FR), and Vega Escondida (VE) in Sierra Bermeja; Alfaguara (AG), Fuente Amargosa (FA), and Balneario de Fuente Amargosa (BFA) in

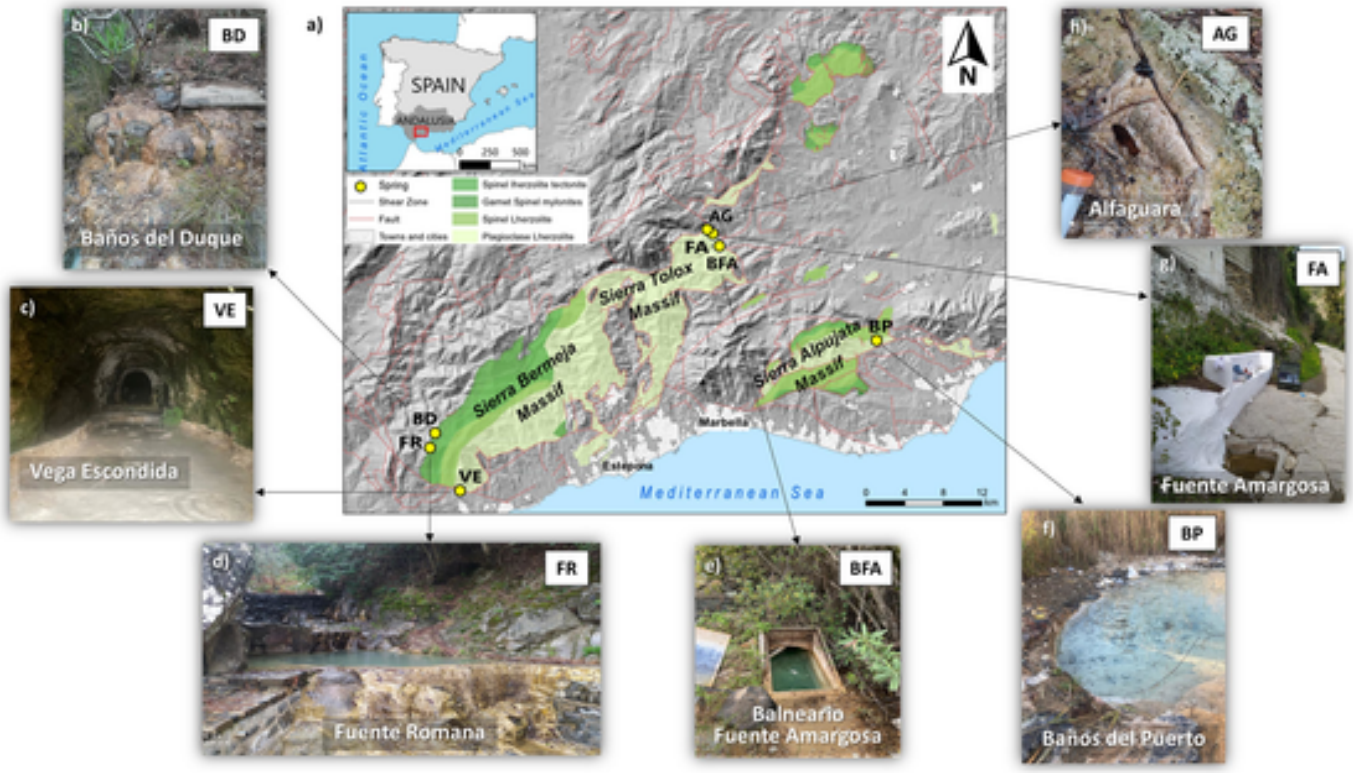

Fig. 1. Geological map showing the tectonometamorphic domains in Ronda peridotites massifs (a) according to Gervilla et al. (2002), with location and overview of the seven serpentinite-hosted hyperalkaline springs studied throughout the Ronda ultramafic massif (Sierra Bermeja and Sierra de Tolox) and the Ojén ultramafic massif (Sierra Alpujata); b) BD: Baños del Duque, c) VE: Vega Escondida, d) FE: Fuente Romana, e) BFA: Balneario Fuente Amargosa, f) BP: Baños del Puerto, g) FA: Fuente Amargosa, and h) AG: Alfaguara. In all seven hyperalkaline springs, samples of groundwater and their associated carbonate (travertine) precipitates were collected and analyzed for the molecular and isotopic composition of organics.

Sierra Tolox; and Baños del Puerto (BP) in Sierra Alpujata. All seven springs are located along or next to fluvial courses or streams corresponding to faults or tectonic contacts between or in the vicinity of peridotites and mafic, metamorphic or metasedimentary rocks (Etiope et al., 2016). The waters, crystalline crusts, travertines, and sediment deposits have been well characterized for their geochemistry, mineralogy and gas composition (Etiope et al., 2016; Giampouras et al., 2019; Ojeda et al., 2023).

Groundwater in the Ronda springs generally discharges from natural springs. However, in FA and BFA water issues from a fountain and a gallery, respectively (Fig. 1e and g). Most sites are fully exposed to light, except VE and BFA that are in the shade (Fig. 1). In VE, water travels several meters through a ~1 m-high gallery before the sampling point (Fig. 1c) and in BFA the spring is protected by a manmade concrete slab (Fig. 1c), only opened at the collection time. The main types of precipitates in the studied sites are travertines forming build-up lithified terraces. In addition, crystalline crusts also occur as thin films floating on the surface of the accumulated or dammed water in the discharge zones of some springs (VE and BFA), while sediments are unconsolidated solid precipitates at the bottom of these water accumulations (Giampouras et al., 2019). Overall, the travertines are mostly composed of calcite, which constitute 100 % of the mineral composition in BP, FA and AG; ca. 76 % in BD and VE; and 33 % in FR. In BFA, the travertines mineralogy is fully represented by aragonite. This mineral is also an important component of the travertine deposits in FR (64 %) and VE (24 %). Other minerals present in the investigated travertines are quartz (22 % in BD and 3 % in FR) and dickite (2 % in BD).

Two types of samples were collected from each of the seven investigated springs: water and associated surface carbonate deposits (travertines). For water sampling, ca. 10 l of water was filtered in-situ using a manual filtrate system (glass fiber filters 0.7 μm, Whatman). For travertine sampling, from 5 to 10 g of precipitates were sampled from the carbonate terraces surrounding the springs by scraping the deposits surface with stainless-steel spatula and tweezers, both previously cleaned with organic solvents (dichloromethane or DCM, and methanol or MeOH). In general, the travertines were sampled from consolidated deposits, except for VE and BFA, where samples were taken from floating crusts of deposits under formations. The filters for water samples were wrapped in previously baked (500 °C for 8 h) aluminum foil and the travertine samples were transferred to polyethylene containers, all stored at 4 °C in the dark until transported to the laboratory.

2.3. Organics extraction and isolation

The travertine samples and water filters (10 l filtered on glass fiber filters 0.7 μm, Whatman) were freeze-dried prior to extraction. After addition of three internal standards (tetracosane-D_{50}, myristic acid-D_{27}, and 2-hexadecanol), extraction was performed with a mixture of DCM and MeOH (9:1 vol/vol) using an ultrasound bath (3 cycles of 10 min each). The three organic extracts (concentrated to 1 ml in a rotavapor) were combined and hydrolyzed overnight at room temperature in methanolic KOH (6 % *w*/w), and then separated into neutral and acidic according to a protocol described elsewhere (Grimalt et al., 1992). Further separation of the neutral fraction into non-polar and polar subfractions was done following the procedure described by (Carrizo et al., 2019). In total, three polarity fractions (i.e. non-polar containing defunctionalized hydrocarbons, polar containing alcohols, and acidic containing carboxylic acids) were obtained for each groundwater and travertine sample.

2.4. Biomarker analysis

Biomarkers were characterized on the three polarity fractions by gas chromatography–mass spectrometry (GC–MS) with an Agilent 8860 series gas chromatograph interfaced with an Agilent 5977 BCE mass selective single-axis detector. The non-polar fraction was directly injected on hexane, while the acidic fraction was previously derivatized with BF_3 in MeOH, and the polar fraction silylated using *N,O*-bis (trimethylsilyl) trifluoroacetamide. A 1-μL aliquot of non-polar and derivatized extracts was injected in splitless mode onto a 60-m DB- 5MS fused-silica column (60-m × 0.25-mm internal diameter and film thickness of 0.25 μm). The GC oven temperature was programmed as follows: 50 °C injection and hold for 1.5 min, ramp at 20 °C min to 160 °C (isothermal hold of 5 min), and ramp at 5 °C min to 315 °C (hold for 10 min). The injector, transfer line, and MS source temperatures were set at 290 °C, 300 °C, and 230 °C, respectively, and the source was operated at 70 eV. Organic compounds were identified based on the comparison of mass spectra with reference materials, and they were quantified based on response factors of representative standards of *n*-alkanes (C_{10} to C_{40}), fatty acids methyl esters or FAME (C_8 to C_{24}), and *n*-alkanols (C_{14}, C_{16}, C_{18}, and C_{20}). Procedural blanks were run in order to monitor background interferences. All chemicals and standards are from Sigma Aldrich (San Louis, Missouri, USA). The recovery of the internal standards was determined at 71 ± 16 %.

2.5. Compound-specific isotopic analysis

Compounds from the three polarity fractions were subsequently analyzed to characterize their isotopic signatures using a gas chromatograph-mass spectrometer (Trace GC 1310 ultra/ISQ QD MS) connected with an isotope-ratio mass spectrometry system (MAT 253 IRMS, Thermo Fisher Scientific). For the GC analysis, the oven temperature program was set to gradually increase from 70 °C to 130 °C at 20 °C·min^{-1}, and to 300 °C at 10 °C·min^{-1} (held for 15 min). Conditions for the IRMS analysis consisted of an electron ionization of 100 eV, Faraday cup collectors of *m/z* 44, 45, and 46, and a temperature of the CuO/NiO combustion interface of 1000 °C. The samples were injected in a PTV injector in splitless mode, with an inlet temperature of 50 °C, and then a ramped temperature of 2.5 °C·*sec*$^{-1}$ until 320 °C (held 2.5 min), using helium as carrier gas at a constant flow of 1.1 ml·min^{-1}. The stable-carbon isotopic composition is expressed as the $\delta^{13}C$ ratio, in per mile notation (‰) and relative to the Pee Dee Beelemite (PDB) standard. Details on the calculation of individual $\delta^{13}C$ values, based on the use of reference materials, and corrections applied for the FAME are provided elsewhere (Sánchez-García et al., 2021). We only report here well-resolved analytes, corresponding to major compounds within the lipid classes.

2.6. Water chemistry

The temperature (±0.4 °C), pH (±0.01), electrical conductivity (±1 %), redox potential (±0,02 mV), and dissolved oxygen (±0,1 mg·l^{-1} from 0 to 8 mg·l^{-1}; ±0,2 when >8 mg·l^{-1}) of the water samples was determined in situ using a portable multi-parameter probe (Hach-Lange HQ40d; Hach, Loveland, CO, USA). For pH measurements, two pH buffers (at pH 7 and pH 10) were used for calibrating the pH electrodes. For the redox potential probe, the Ag/AgCl reference electrode with a 3 M KCl solution and a redox standard solution were used to calibrate the sensor. The physico-chemical features measured in the groundwater samples from the seven Ronda hyperalkaline springs (Table 1) were comparable to those recorded in other sampling campaigns (Etiope et al., 2016; Ojeda et al., 2023).

3. Results and discussion

3.1. Detection of biogenic organics in groundwater and associated travertines in the serpentinization-hosted hyperalkaline springs of Ronda

A variety of solvent extractable organic compounds were detected in the seven hyperalkaline springs of Ronda (*n*-alkanes, isoprenoids, diploptene, alkanoic acids, *n*-alkanols, sterols, phytol, farnesol, or diplopterol; Table 2) in the non-polar (*Database S1*), acidic (*Database S2*), and polar (*Database S3*) fractions. Among them, we detected molecular and isotopic fingerprints of life in form of lipid biomarkers (i.e. cell membrane-derived compounds), which were always found in higher concentration in the travertine (μg·g^{-1} or ppm) than groundwater (μg·l^{-1} or ppb, and ng·l^{-1} or ppt) samples (Table 2).

For instance, we identified linear hydrocarbon with functional groups such as -COOH (i.e. *n*-alkanoic acids) or -OH (i.e. *n*-alkanols). Linear and saturated (a.k.a. *normal*) carboxylic acids (i.e. *n*-alkanoic acids) and alcohols (i.e. *n*-alkanols) are straight hydrocarbons incorporating a terminal carboxyl or hydroxyl group, respectively, that compose the non-polar chains of the amphipathic lipid bilayer of the cells of any organism to delimit it from its environment (Summons et al., 2021). In the Ronda hyperalkaline springs, *n*-alkanoic acids (C_{10}-C_{30}) and *n*-alkanols (C_{12}-C_{30}) were detected in both groundwater and travertine samples (Table 2, and *Database S2-S3*), with a biogenic molecular pattern showing a few individual peaks (i.e. the C_{16} and C_{18} *n*-alkanoic acids; and the C_{18}, C_{22}, C_{24}, or C_{28} *n*-alkanols) standing out from their homologous (Fig. 2a-d). Regardless of the specific peaks, even-numbered carbons dominated both the *n*-alkanoic acid (*Fig. S1*) and *n*-alkanol (*Fig. S2*) series in the groundwater and travertine samples, a consistent indication of biogenicity. The characteristic even/odd pattern in biologically synthesized lipid chains stems from the enzymatic-driven incorporation of carbon atoms in pairs (Batsale et al., 2021). Both the *n*-alkanoic acids (a.k.a. *n*-fatty acids when biogenic) and *n*-alkanols were detected at higher concentration in the travertine (μg·g^{-1}) than groundwater (μg·l^{-1} the acids and ng·l^{-1} the alkanols) samples (Table 2 and Fig. 2a-d). The compounds biogenicity was supported by carbon isotopic signatures depleted in ^{13}C (i.e. negative values of the $\delta^{13}C$ ratio) for both the *n*-alkanols (i.e. -20.3 to −36.0 ‰), and the *n*-fatty acids in groundwater (−13.3 to −29.8 ‰) and travertine (−14.6 to −39.5 ‰) samples (Fig. 3). Biologically synthesized hydrocarbons are typically depleted in ^{13}C as a result of the enzymatic preference towards

Table 1
Physico-chemical characteristics of the serpentinization-driven hyperalkaline springs of Ronda (see Fig. 1 for details on the geographical distribution of the springs). Temp is temperature, EC electrical conductivity, E_h redox potential, and DO dissolved oxygen.

Peridotite massif	Sierra	Serpentinization-driven spring	Site ID	Temp	pH	EC	E_h	DO
				°C		μS·cm^{-2}	mV	mg·l^{-1}
Ronda ultramafic massif	Bermeja	Baños del Duque	BD	17.2	11.6	539	−174	2.1
		Fuente Romana	FR	14.3	12.0	537	−150	2.4
		Vega Escondida	VE	19.0	12.2	1389	−272	2.0
	Tolox	Balneario Fuente Amargosa	BFA	13.0	10.2	257	−32	6.5
		Fuente Amargosa	FA	17.9	11.6	1256	−275	1.8
		Alfaguara	AG	16.9	11.8	1160	−230	2.0
Ojén ultramafic massif	Alpujata	Baños del Puerto	BP	20.5	11.4	666	−165	0.2

Table 2
Concentration and molecular distribution of organics in groundwater and travertine samples from the seven Ronda hyperalkaline springs (see Table 1 or Fig. 1 for the site acronyms). Concentration is expressed in μg·g^{-1} (ppm) of dry weight in the travertine samples, and in μg·l^{-1} (ppb) in the groundwater samples, except for compounds of the polar fraction (ng·l^{-1} or ppt), which are marked with asterisks.

Compound, ratio or proxy	Other name or acronym	Water samples (μg·l^{-1}, except alcohols*: ng·l^{-1})							Travertine samples (μg·g^{-1} dry weight)						
		BD	FR	VE	BP	BFA	FA	AG	BD	FR	VE	BP	BFA	FA	AG
Sum of *n*-alkanes	C_{12}-C_{36}	3.7	4.3	4.0	3.4	4.9	4.3	4.8	19	5.8	1.1	1.6	0.7	17	10
2,6,10-Trimethylpentadecane	Norpristane	0.06	0.07	0.08	0.04	0.06	0.08	0.07	0.11	n.d.	0.01	0.01	0.01	0.12	0.14
2,6,10,14-Tetramethylpentadecane	Pristane	0.10	0.12	0.14	0.10	0.13	0.18	0.18	0.24	0.09	0.03	0.03	0.02	0.29	0.33
2,6,10,14-Tetramethylhexadecane	Phytane	0.10	0.13	0.13	0.10	0.11	0.16	0.14	0.36	0.16	0.03	0.03	0.02	0.26	0.26
2,6,10,15,19,23-Hexamethyl-2,6,10,14,18,22-tetracosahexaene	Squalene	0.04	n.d.	0.05	0.04	n.d.	n.d.	0.06	0.91	0.39	0.17	0.05	0.02	0.62	1.4
Sum of monomethyl alkanes	C_{15}-C_{29}	0.61	0.65	0.61	0.53	0.63	1.2	0.72	3.6	1.9	0.11	0.58	0.06	1.9	2.2
Sum of alkenes	C_{15}-C_{20}	0.05	0.06	0.07	0.06	0.06	0.06	0.08	2.6	1.3	0.02	0.11	0.01	0.15	0.72
Sum of hopanoids	C_{27}-C_{35}	0.02	0.01	0.02	0.01	0.02	0.15	0.01	n.d.	n.d.	n.d.	n.d.	n.d.	n.d.	n.d.
22(29)-Hopene	Diploptene	n.d.	n.d.	n.d.	n.d.	n.d.	n.d.	n.d.	1.5	n.d.	n.d.	n.d.	n.d.	n.d.	n.d.
Sum of *n*-fatty acids	C_{10}-C_{30}	24	24	20	17	61	18	23	150	12	1.0	35	0.23	19	19
Sum of *iso/anteiso* fatty acids	*i/a*-(C_{13}-C_{21})	0.33	0.33	0.45	0.35	1.1	0.21	0.28	8.8	1.1	0.07	2.0	0.17	3.2	4.6
Other monomethyl fatty acids	Me-(C_{14}-C_{18})	n.d.	n.d.	n.d.	n.d.	n.d.	n.d.	n.d.	3.7	n.d.	0.01	n.d.	n.d.	0.2	n.d.
Sum of monounsaturated fatty acids	MUFA	1.4	1.5	1.9	0.91	4.2	1.1	1.0	36	18	0.49	7.9	0.36	7.5	17
Sum of polyunsaturated fatty acids	PUFA	0.06	0.08	0.21	0.05	0.25	0.09	0.08	16	13	0.05	1.5	0.01	0.48	1.1
Sum of *n*-alkanols	C_{12}-C_{30}	9.2*	9.1*	1.9*	13*	21*	16*	14*	15	2.2	0.06	3.8	0.002	4.2	8.1
Sum of alkenols	C_{18}-C_{24}	0.72*	0.51*	0.45*	1.5*	1.2*	1.5*	1.3*	1.1	0.26	0.002	0.16	<0.001	0.34	0.48
Sum of phytosterols[a]	C_{27}-C_{29}	0.46*	0.51*	0.10*	0.53*	2.4*	0.85*	0.65*	13	1.5	<0.001	29	0.046	16	16
Sum of other sterols[b]	C_{27}-C_{29}	0.88*	0.23*	0.32*	1.5*	2.1*	0.36*	0.86*	4.0	0.69	0.004	5.5	0.03	6.2	11.2
3,7,11,15-Tetramethyl-2-hexadecen-1-ol	Phytol	n.d.	n.d.	n.d.	n.d.	n.d.	n.d.	n.d.	6.9	3.3	0.005	6.1	n.d.	2.6	1.8
3,7,11-Trimethyl-2,6,10-dodecatrien-1-ol	Farnesol	n.d.	n.d.	n.d.	n.d.	n.d.	n.d.	n.d.	n.d.	n.d.	n.d.	n.d.	n.d.	n.d.	0.07
17β(H),21β(H)-22-Hydroxyhopane	Diplopterol	n.d.	n.d.	n.d.	n.d.	n.d.	n.d.	n.d.	1.6	1.4	0.01	0.36	0.03	0.68	0.38
Carbon preference index (C_{23}-C_{35} *n*-alkanes)	CPI	1.0	1.0	1.1	1.0	1.0	1.1	1.0	2.5	2.2	1.7	1.8	1.0	1.3	1.4

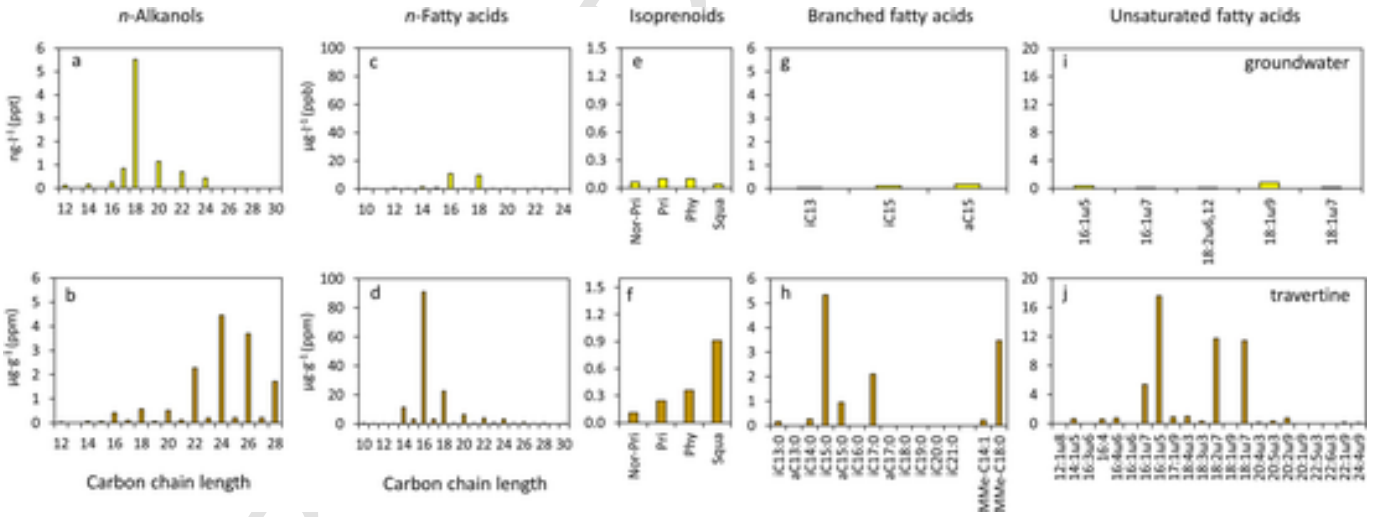

Fig. 2. Comparison of the variety and concentration (ppb/ppt vs ppm) of biomarkers in groundwater (top row) and travertine (bottom row) samples; a-b) linear and saturated alkanols, c-d) linear and saturated fatty acids, e-f) isoprenoids, g-h) monomethylated fatty acids (*iso*- or i- when the methyl group is in the N-1 position, and *anteiso*- or a- in the N-2 position), i-j) fatty acids containing double bonds (as many as the number indicated after the colon, and in the position indicated by the number after the ω). For all compounds (a-j), data from the BD spring as representative of the quantitative difference (variety and concentration) between groundwater and travertine samples. The numbers in the X-axis indicate to the total number of carbons in the chain. In e-f, Nor-Pri stands for norpristane, Pri for pristane, Phy for phytane, and Squa for squalene.

the energetically favorable ^{12}C relative to its heavier isotope (^{13}C) during carbon fixation (Schidlowski, 2001).

We also detected isoprenoids, a family of methylated alkanes formed by elongation of repeating C_5 isoprene units that compose archaeal membrane lipids (Kates, 1993), the side chain of chlorophyll-a in phototrophs (Didyk et al., 1978), or tocopherols in plants and phytoplankton (Goosens et al., 1984). Therefore, isoprenoids are unambiguous biomarkers and here we specifically identified them in the form of phytane, pristane, nor-pristane, and squalene (*Database S1*) in both groundwater and travertine samples, with lower concentration in the former (Fig. 2e-f). All isoprenoids showed fairly negative $\delta^{13}C$ values characteristic of biogenic sources in both groundwater (−26.0 to −28.5 ‰) and travertine (−22.3 to −34.3 ‰) samples (*Fig. S3*).

Additional compounds of unambiguous biogenic origin that we detected in Ronda were branched (i.e. monomethylated) and unsaturated (i.e. containing double bonds) fatty acids, phytol, neophytadiene, diplopterol, and sterols (i.e. rigidifying components of eukaryotic cell membranes) (Table 2). Some of these compounds (monomethyl fatty acids of *iso/anteiso* configuration from C_{13} to C_{21}) are generally associated with bacteria (Kaneda, 1991), whereas some of them (*iso/anteiso*-C_{15} and C_{17} fatty acids) are more specifically related to sulfate-reducing bacteria (Russell et al., 1997). Sulfate reduction is an anaerobic metabolism conducted by different organisms belonging to classes like

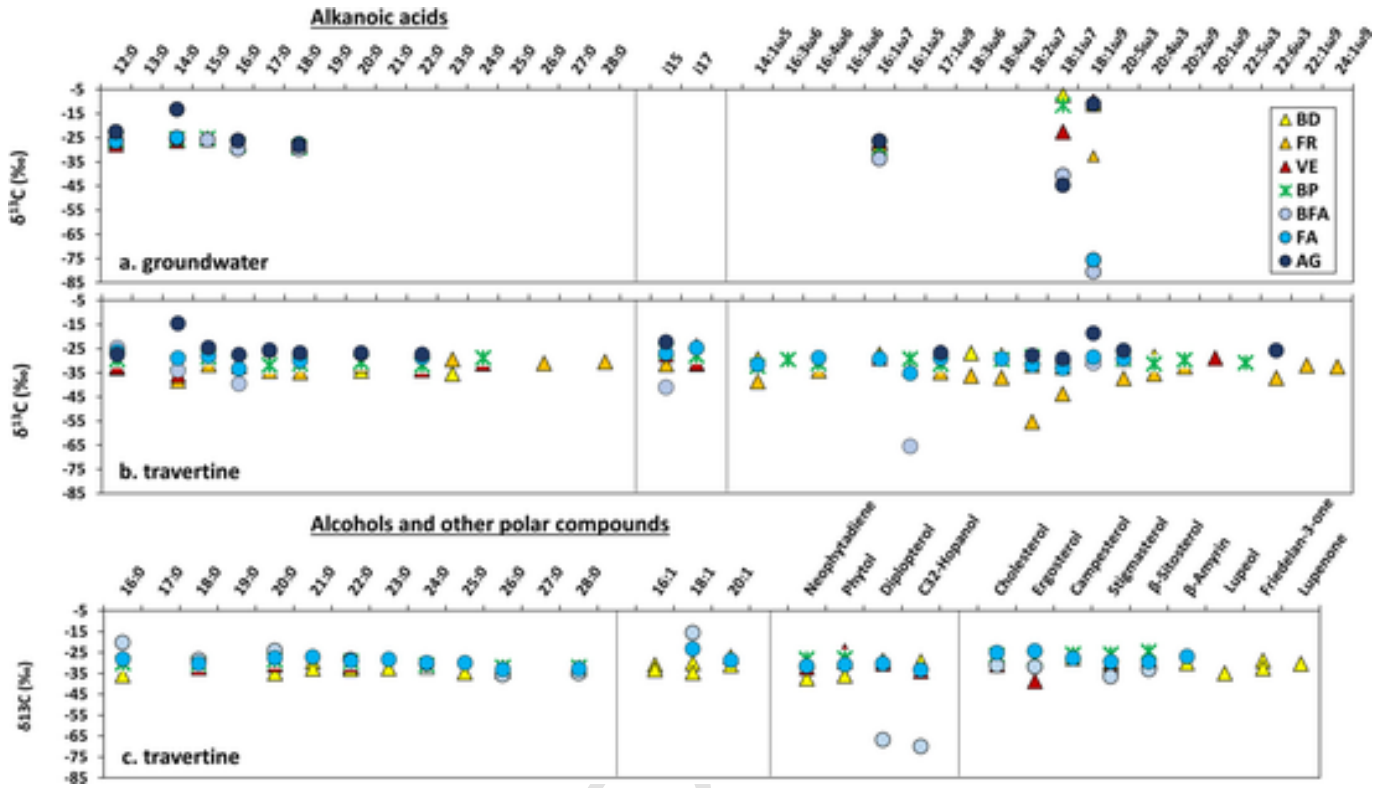

Fig. 3. Compound-specific isotopic composition ($\delta^{13}C$) of the organic compounds identified in the acid (a-b) and polar (c) fractions of groundwater (a) and travertine (b-c) samples from the seven hyperalkaline springs of the Ronda peridotites. These isotopic fingerprints can be interpreted in a carbon metabolism context, where different fixation pathways produce characteristic $\delta^{13}C$ values ranging from ca. -19 to −34 ‰ for the Calvin Cycle (Hayes, 2001), −12 to −21 ‰ for the reverse tricarboxylic acid pathway (Preuß et al., 1989), −4 to −15 ‰ for the 3-hydroxypropionate bicycle (Hayes, 2001), −8 to −12 ‰ for both the 3-hydroxypropionate/4-hydroxybutyrate (3HP/4HB) bicycle or the dicarboxylate-4-hydroxybutyrate (DC-4HB) pathways (Berg et al., 2010; House et al., 2003), −28 to −44 ‰ for the Wood-Ljungdahl pathway (Preuß et al., 1989), and ≪−40 ‰ for methanogenic/methanotrophic metabolisms (Whiticar, 1999).

Clostridia (*Firmicutes*) and δ-*Proteobacteriota*, or the phyla *Thermodesulfobacteriota*, *Euryarchaeota*, or *Crenarchaeota* (Muyzer and Stams, 2008), which have been described in diverse serpentinite-hosted microbial communities worldwide (Suzuki et al., 2013; Mottl et al., 2003; Brazelton et al., 2010, 2012; Tiago and Veríssimo, 2013). In the Ronda springs, *iso/anteiso* fatty acids were detected in both the groundwater and travertine samples (Table 2), with higher relative abundance in the latter (Fig. 2g-h, and *Database S2*).

Other detected compounds were biomarkers of phototrophs, such as unsaturated (i.e. 16:1ω7, 18:2ω6, 20:4ω3, 20:5ω3 and 22:6ω3) fatty acids (*Database S2*), which are related to cyanobacterial and/or microalgal sources (Dijkman et al., 2010). Further, phytosterols such as β-sitosterol, campesterol and stigmasterol mostly derived from eukaryotic phototrophs (plants and algae; Goad and Akihisa, 1997; Volkman, 1986) were also detected in the Ronda hyperalkaline springs (Table 2). All phototrophic biomarkers were more concentrated in the travertine than groundwater samples, by 3 (fatty acids; *Database S2*) or 6 (phytosterols; *Database S3*) orders of magnitude of difference. The relative abundance of phototrophic biomarkers in the travertine deposits was consistent with the abundant detection of phytol, the esterifying alcohol of cyanobacterial and green-plant chlorophylls (Didyk et al., 1978) in all travertine samples except VE and BFA (Table 2). In these two springs, groundwater emerges in a closed environment protected from solar radiation either by a semi-closed gallery (VE) or a concrete lid (BFA) (Fig. 1c and e), which could explain the paucity of phototrophs.

The relevance of phototrophic activity in the Ronda springs was confirmed by the compound-specific isotopic analysis of the identified biomarkers that recorded ^{13}C-depleted signatures broadly compatible with the Calvin Cycle ($\delta^{13}C$ of ca. -19 to −34 ‰; Hayes, 2001) both in the acid (Fig. 3a-b) and polar (Fig. 3c) fractions. The Calvin Cycle is a metabolism used by phototrophs such as cyanobacteria, purple sulfur and non-sulfur bacteria, algae or plants (Hügler and Sievert, 2011) to fix inorganic carbon and generate biomass. The presence of phototrophic biomarkers in the Ronda springs (more abundant in the travertine than groundwater samples) was consistent with the report of microbial phototrophs from the *Cyanobacteria* phyla, as well as the α, β, or γ-*Proteobacteria* classes in different continental serpentinite-hosted alkaline seeps from Portugal (Tiago and Veríssimo, 2013), Canada (Brazelton et al., 2012), or California (Suzuki et al., 2013), based on 16S rRNA gene sequences and metagenomics. Notably, Suzuki et al. (2013) described a genus of the β-proteobacterial order *Burkholderiales* (i.e. *Hydrogenophaga*) that conducted the Calvin Cycle oxidizing hydrogen as a source of energy (Brazelton et al., 2012).

The molecular profile of bacterial biomarkers in the Ronda peridotites was overall comparable to those in oceanic serpentinization counterparts. For instance, in Lost City different works (Bradley et al., 2009; McCollom and Seewald, 2007; Mehay et al., 2013) have described similar series and concentrations of *n*-fatty acids (C_{14} to C_{26}; 1 to 320 $\mu g \cdot g^{-1}$), monounsaturated fatty acids such as 16:1 and 18:1 (0.02 to 0.85 $\mu g \cdot g^{-1}$), diplopterol (0.02 to 1.5 $\mu g \cdot g^{-1}$), or C_{27} to C_{30} sterols (0.01 to 0.58 $\mu g \cdot g^{-1}$) as those reported here. However, in contrast to the ocean-floor hydrothermal ecosystem at the Middle-Atlantic Ridge, no archaea-specific biomarkers (e.g. archaeol and other isoprenoidal diethers, or isoprenoid hydrocarbons such as pentamethylicosane and derivatives) were detected in Ronda. Furthermore, the compound-specific isotopic signatures in Lost City were considerably more ^{13}C-enriched (i.e. more positive $\delta^{13}C$; Bradley et al., 2009; McCollom and Seewald, 2007; Mehay et al., 2013) than the equivalent bacterial biomarker in Ronda (e.g. $\delta^{13}C_{n\text{-fatty acids}}$ from −32.1 to −1.2 ‰ in Lost City versus −39.5 to −13.3 ‰ in Ronda; or $\delta^{13}C_{diplopterol}$ from −20.4 to −16 ‰ in

Lost City versus −66.9 to −28.8 ‰ in Ronda). Yet, eukaryotic biomarkers such as cholesterol and phytosterols showed comparable isotopic signatures in Ronda ($\delta^{13}C$ from −36.6 to 24.6 ‰) and Lost City ($\delta^{13}C$ from −29 to 25.3 ‰). Therefore, the serpentinization-hosted ecosystem in Ronda seems to be dominated by bacteria and phototrophic eukaryotes, in contrast to the ocean-floor hydrothermal ecosystem in Lost City, largely represented by methane-cycling archaeal communities according to their relative abundance of archaeal lipids.Besides the Calvin Cycle, the wide range of $\delta^{13}C$ recorded for the identified compounds from the acidic (−7.3 to −80.6 ‰) and polar (−15.6 to −70.0 ‰) fractions (Fig. 3) pointed towards the contribution of additional metabolisms to the synthesis of lipid biomarkers. The most enriched $\delta^{13}C$ values (i.e. $\delta^{13}C$ ca. ≥−15 ‰) observed in the Ronda fatty acids (Fig. 3a-b) and alcohols (Fig. 3c) could be explained by the use of i) the reverse tricarboxylic acid (rTCA) pathway ($\delta^{13}C$ from −12 to −21 ‰; Hayes, 2001), ii) the 3-hydroxypropionate (3HP) bicycle ($\delta^{13}C$ from −4 to −15 ‰; Hayes, 2001); and/or iii) the 3-hydroxypropionate/4-hydroxybutyrate (3HP/4HB) bicycle and/or the dicarboxylate-4-hydroxybutyrate (DC-4HB) pathways ($\delta^{13}C$ from ca. -8 to −12 ‰; Berg et al., 2010). Potential users of these pathways are microorganisms from *Nitrospirae*, *Aquificae*, *Chlorobiales*, or ε-*Proteobacteria* (rTCA pathway); *Chloroflexi* (3HP bicycle); or *Crenarchaeota* (3HP/4HB and/or DC-4HB pathways). Most of these taxa (*Chloroflexi*, *Aquificae*, ε-*Proteobacteria*, or the crenarchaeal order *Desulfurococcales*) have been indeed described in diverse serpentinizing-hosted microbial communities (Suzuki et al., 2013; Brazelton et al., 2010; Tiago and Veríssimo, 2013) and might also be involved in the biosynthesis of the most ^{13}C-enriched biomarkers in the Ronda samples.

Finally, the most ^{13}C-depleted biomarkers (−38.6 to −80.6 ‰; Fig. 3) denoted the participation of metabolisms such as methanotrophy and/or Wood-Ljungdahl pathway (Preuß et al., 1989; Whiticar, 1999; Hayes, 2001). These metabolisms, which are further discussed in the following section, are conducted by methanotrophs, acetogens, and/or fermenters (Hügler and Sievert, 2011). Altogether, the molecular and isotopic compositions of the described biomarkers allowed us recreate the serpentinization-hosted ecosystem in the Ronda hyperalkaline springs (Fig. 4), with different contributions of specific microbial sources and associated metabolisms depending on the hyperalkaline spring (*Fig. S4*).

3.2. Biogenic production and consumption of methane in two of the seven serpentinizing-hosted springs. Implications for the search of Martian life

Some organics (iso-C_{15}, 14:1ω5, 16:1ω8, 18:1ω8, 18:1ω7 or 18:2ω7 fatty acids; and diplopterol and a C_{32} hopanol) displayed $\delta^{13}C$ values as depleted as −38.6 to −80.6 ‰ (Fig. 3), which suggested the contribution of metabolisms involving acetogenic activity via the Wood-Ljungdahl pathway ($\delta^{13}C$ from −28 to −44 ‰; Preuß et al., 1989) and the consumption of methane by methanotrophs ($\delta^{13}C$ from ca. −40 to −120 ‰; Whiticar, 1999). Representative users of the Wood-Ljungdahl pathway in the Ronda springs could be *Firmicutes*, δ-*Proteobacteria*, or *Spirochaetes* (Hügler and Sievert, 2011). In fact, *Clostridia* (typically order *Clostridiales*) appears to be a common taxon of serpentinite-hosted

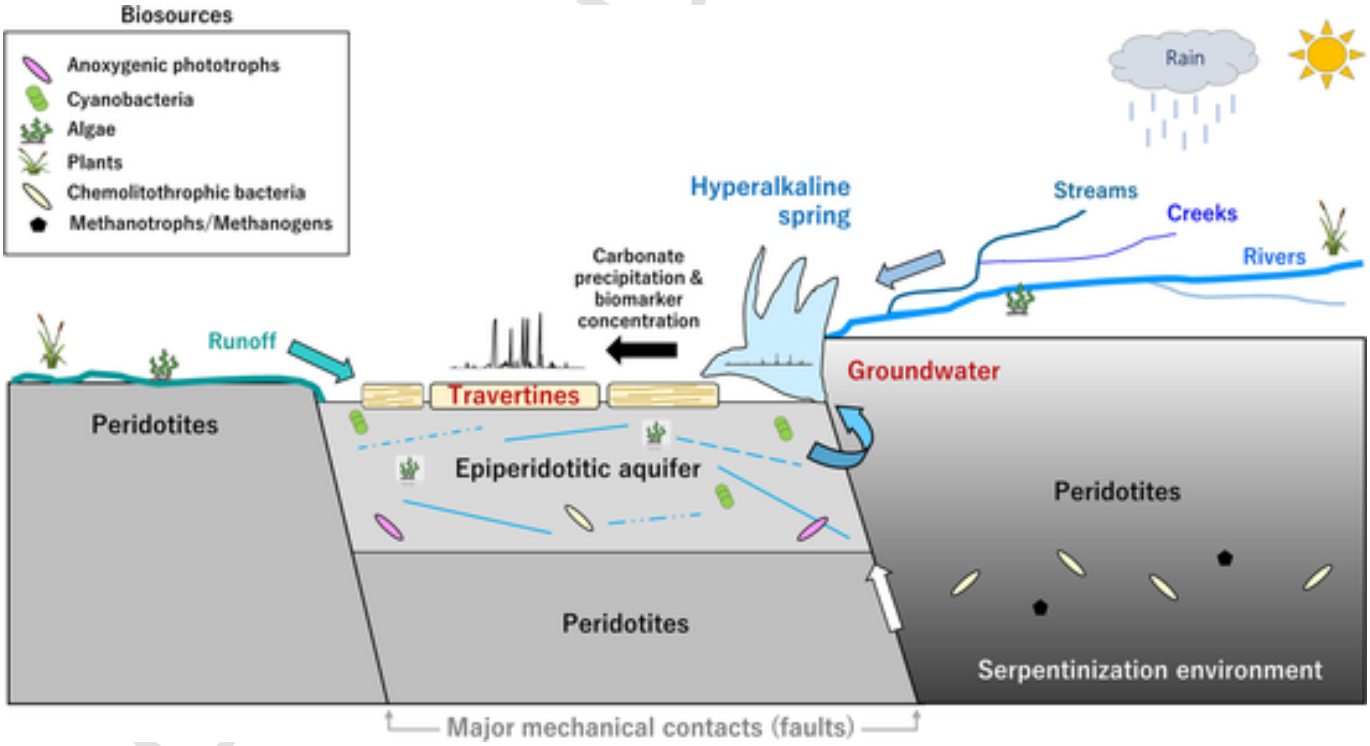

Fig. 4. Schematic illustration of the geological setting of the Ronda peridotites and the associated serpentinization-hosted ecosystem, with the main biological sources contributing to the biomarker record of groundwater and travertine samples in the seven hyperalkaline springs studied. The biological sources inferred from the molecular and isotopic composition of lipid biomarkers (see *Fig. S4* for details on the prevailing carbon metabolisms and ecological differences between the seven springs) are summarized in the legend. The biomarker record in groundwater and travertine samples is symbolized by chromatograms with higher and more varied peaks in the latter, as a consequence of the biomarker concentration during the carbonate precipitation at the surface. The blue water jet and beige layered deposits represent the groundwater and travertine samples in any of the seven hyperalkaline springs. The colored arrows represent the different water inputs in the hyperalkaline springs: deep water rising from the serpentinization environment (straight white arrow); water from subsurface or relatively shallow flows (epiperidotitic aquifer) that mixes with deep groundwater before emerging as a hyperalkaline spring (blue bending arrow); mix of surficial waters from rainfall, rivers, streams, creeks, etc. (straight blue arrow); and runoff water (green-bluish arrow). The black straight arrow represents the biomarker concentration from groundwater to travertine deposits by accumulation over time of traces of life both prokaryotic and eukaryotic organisms, autochthonous and autochthonous sources, and from subsurface and surface.

ecosystems (Suzuki et al., 2013; Tiago and Veríssimo, 2013), normally inhabiting the deepest and most anoxic regions of the subsurface underlying hyperalkaline springs (Brazelton et al., 2012). This taxon is suspected to conduct sulfate reduction and, although also capable of autotrophic or mixotrophic growth (Sorokin et al., 2008), it possesses genes for hydrogen production typically associated with fermentation (Brazelton et al., 2012). Fermentation is a metabolic strategy that can involve the use of a single organic compound as both oxidant and reductant, particularly advantageous in extreme environments such as those hosted by serpentinization, where exogenous oxidants (i.e. electron acceptors) are scarce (Schrenk et al., 2013). In the Ronda peridotites as in other ultramafic serpentinizing-hosted environments, the release of large amounts of H_2, CH_4, and other hydrocarbons including small organic compounds (McCollom and Seewald, 2007) could be feeding a microbial community largely built on fermentation, methanogenesis and methanotrophy, as well as hydrogenotrophy.

The most ^{13}C-depleted compounds (−66.9 to −80.6 ‰) detected in the Ronda springs (Fig. 3) have been described as biomarkers of methanotrophs type I from the *γ-Proteobacteria* class (16:1ω8 fatty acid) and type II from *α-Proteobacteria* class (18:1ω8 fatty acid) (Bowman et al., 1991). The two ^{13}C-depleted polar compounds (i.e. diplopterol and a C_{32} hopanol) have been related to prokaryotes in general (Brocks and Summons, 2003), and to a variety of aerobic and anaerobic bacteria in particular (Rohmer et al., 1984; Sinninghe Damsté et al., 2007). Interestingly, such ^{13}C-depleted biomarkers were detected in groundwater and travertine samples from BFA and FA (Fig. 3), both springs from Sierra de Tolox (Fig. 1). The very negative $\delta^{13}C$ values imply biological sources of microorganisms utilizing (i.e. oxidizing) methane, since it is the only natural carbon substrate commonly found with such ^{13}C depleted signatures (Elvert et al., 1999). Notably, in the two BFA and FA springs Etiope et al. (2016) measured $\delta^{13}C$ values for outgassing CH_4 that were considerably more depleted (−54.5 to −68.5 ‰) than in the other hyperalkaline springs of the region (−10.6 to −28.8 ‰). Etiope and coworkers explained the very negative $\delta^{13}C$ values for CH_4 in FA and BFA by the mixture of biogenic (i.e. microbial methanogenesis and/or thermogenic degradation of organic matter) and abiotic (i.e. via Fischer Tropsch-type reactions) sources contributing to the gas production. Accordingly, we interpret that the ^{13}C-depleted lipids in BFA and FA (i.e., 16:1ω8 and 18:1ω8 acids, diplopterol and C_{32} hopanol) must derive from microorganisms growing on (at least) partially biogenic methane (i.e. methanotrophs). The lack of detection of biomarkers for CH_4-metabolizing archaea such as isoprenoidal diethers (e.g. archaeol and derivatives) or pentamethylicosanes, such as those reported in oceanic serpentinization settings (e.g. Bradley et al., 2009; Mehay et al., 2013), led us to think of a methanotrophic activity dominated mainly by bacteria in BFA and FA. The relative depletion in ^{13}C of the identified lipids (−66.9 to −80.6 ‰) relative to the methane substrate (i.e. -54.5 to −68.5 ‰; Etiope et al., 2016) in the BFA and FA springs would reflect the isotope effect accompanying the methane consumption, since microbial incorporation of methane-derived carbon into cellular biomass involves ^{13}C depletion in the synthesized biomass (Elvert et al., 1999). Other metabolic options such as the anaerobic oxidation of methane by a syntrophic association of sulfate-reducing bacteria with methanotrophic archaea using the reverse methanogenesis pathway (Skennerton et al., 2017) were discarded, given the distinct $\delta^{13}C$ values measured for the biomarkers of sulfate-reducing bacteria (i.e. *i*-C_{15} and *i*-C_{17} fatty acids) and methanotrophs (i.e. 16:1ω8 and 18:1ω8 acids, diplopterol and C_{32} hopanol), that is −27.3 to −41.0 ‰ versus −66.9 to −80.6 ‰, respectively (Fig. 3). In sum, methanotrophy largely dominated by bacteria appears to be a present metabolism in BFA and FA, in contrast to the other Ronda springs (BD, VE, FR, BP and AG) lacking of methanotrophy biomarkers and displaying less negative $\delta^{13}C$ values (Fig. 3).

The molecular and isotopic fingerprints of methanogenic/methanotrophic activity in two of the serpentinization-driven springs of Ronda (BFA and FA) are relevant for the search for life on Mars. This planet has hosted serpentinization processes in early times, and anomalously depleted carbon isotopic values (less than −70 ‰) have been measured in the evolved CH_4 from sedimentary rocks and eolian sediments at Gale crater (House et al., 2022). Although the origin of the strongly ^{13}C-depleted methane on Mars has not been clarified yet, one of the possible explanations that have been put forward is the photolysis of biological methane released from the planet's subsurface. Further, microbial methanotrophy, a process in principle energetically favorable under the overall oxidizing Martian atmosphere (House et al., 2022), has been proposed as a possible metabolism for recent and ancient Mars (House et al., 2011). However, both hypotheses of Martian methanogenesis and methanotrophy encounter some inconsistencies yet unresolved. For example, the inorganic CO_2 fueling that microbial ecosystem would need to have a much more ^{13}C-depleted composition than the present Martian atmosphere (i.e. +46 ‰; Webster et al., 2013), and there is no supporting sedimentological evidence for microbial methanotrophy on the Martian surface (House et al., 2022). Clarifying the origin of the Martian depleted methane would require, among other things, the acquisition of carbon isotopic data from Martian regolith, for instance on terrains influenced by past serpentinization. In the absence of direct access to Martian samples in the short term, obtaining data from analogous environments on Earth provides insights to interpret putative biosignatures in serpentinizing systems on Mars. The detection in the Ronda hyperalkaline springs of lipid biomarkers with carbon isotopic signatures as depleted as those reported for evolved CH_4 on sediments from Gale crater (House et al., 2022) opens the door to the possibility that such isotopic fingerprints are related to a methane metabolism on Mars. Obtaining carbon isotopic information from this and other Martian analogs on Earth will enhance our understanding of the carbon cycle on Mars.

3.3. Relevance of serpentinization-associated travertine deposits as geological archives of a possible serpentinization-hosted life on Mars

The concentration and variety of organics in the Ronda hyperalkaline springs were higher in the travertine than in the groundwater samples (Fig. 2). Further, the origin of some of the organics was different in each type of samples, according to their molecular and isotopic profiles. For instance, in all groundwater samples, the series of linear and saturated hydrocarbons with no functional groups or branches (i.e. *n*-alkanes) displayed a normal or Gaussian distribution usually around C_{22}-C_{23} (*Fig. S5*) with a systematic decline of peak abundance with the increase or decrease of the number of carbon atoms in the chain (Fig. 5a), which is characteristic of abiotic or thermally mature organic matter (McCollom and Seewald, 2007). In contrast, in the travertine samples, the same Gaussian distribution of *n*-alkanes was observed in the background but with the coexistence of a few larger peaks (Fig. 5b) that denoted biogenic inputs. The peaking compounds were always odd carbon chains (Figs. 5a and *S5*) usually associated with phototrophs, such as cyanobacteria and/or microalgae (*n*-C_{15}, or *n*-C_{17}) (Shiea et al., 1990; Coates et al., 2014) or land plants (*n*-C_{27}, *n*-C_{29} or *n*-C_{31}) (Hedges and Prahl, 1993). In the biological synthesis of lipid chains, the enzymatic incorporation of carbon atoms in pairs (Batsale et al., 2021) generates molecular distributions of *n*-alkanes with a characteristic odd-even dominance.

The different molecular pattern in the travertine versus groundwater samples was assessed through the carbon preference index (CPI), a measure of the odd dominance of a suite of alkanes used to help determine the biological origin, the maturity of sediments, oils and source rock extracts and/or the paleoenvironmental conditions (Peters et al., 2005). Fresh, biogenic *n*-alkanes typically show CPI values larger than 1 (Peters et al., 2005). In contrast, abiotic *n*-alkanes such as those synthesized in laboratory experiments through Fischer-Tropsch reactions at different temperature (from 100 to 400 °C) show no carbon number

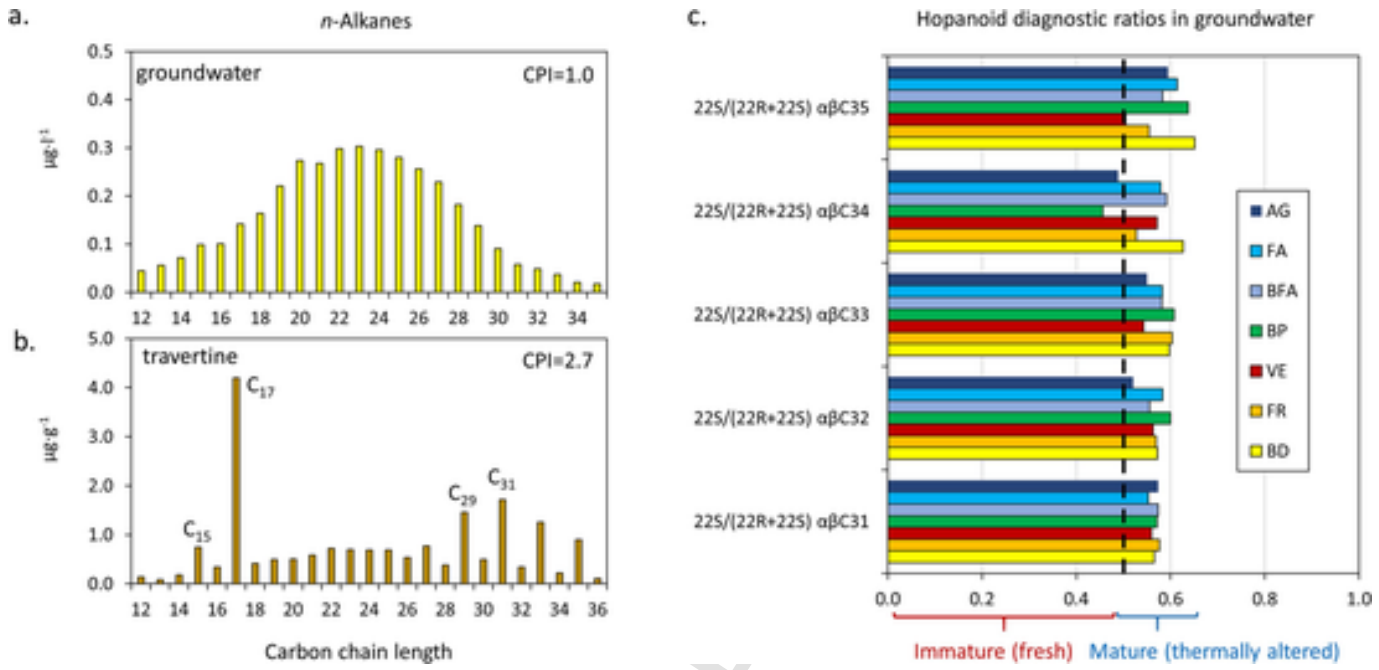

Fig. 5. Recognition of biogenicity in organic molecular patterns from water and travertine samples from the Ronda hyperalkaline springs and maturity level of the αβ hopanes detected only in groundwater. Molecular distribution of *n*-alkanes in the a) groundwater and b) travertine samples of the BD spring (see Fig. 1 for sample location and details), as representative examples of the characteristic normal or Gaussian distributions of abiogenic *n*-alkanes (a), versus uneven distributions indicative of biogenic inputs that show some peaks standing out from the rest of *n*-alkanes (b) observed in all seven springs except BFA (*Fig. S5*). c) Bar plot of the 22S/(22S + 22R) ratio calculated for the five homohopanes (C_{31}-C_{35}) of αβ stereochemistry detected in the seven groundwater samples (see Fig. 1 for naming details), with values generally >0.5 denoting an advanced maturity or aging of the prokaryotic biomarkers (*Fig. S6*).

predominance, thus producing CPI ~ 1 (Rushdi and Simoneit, 2001). Alternatively, biogenic *n*-alkanes can overcome thermal alteration during catagenesis, where long-chain alkanes are randomly cleaved to form shorter homologues (Peters et al., 2005). As a consequence, the characteristic predominance of odd congeners is lost, resulting into decreasing CPI values that tend to approach 1 with increasing maturity (Peters et al., 2005). In the Ronda hyperalkaline springs, the relatively high CPI values in all travertine samples (1.3–2.7) except BFA (Table 2 and *Fig. S5*) illustrate the predominance of odd over even *n*-alkanes characteristic of biogenic organic matter (Sephton, 2014). In contrast, CPI values close to 1 in all groundwater samples and the BFA travertine (Table 2 and *Fig. S5*) suggest either an abiogenic origin (e.g. Fischer-Tropsch type reactions) and/or thermal alteration of biogenic organics. Contribution from biogenic sources to the *n*-alkanes was supported by considerably depleted $\delta^{13}C$ values (−24.7 to −34 ‰; *Fig. S3a*) such as those characteristic of phototrophic bacteria, algae and C3 plants (Hayes, 2001). Although the range of $\delta^{13}C$ variability in the groundwater *n*-alkanes was slightly narrower than that in those of travertine samples (−24.2 to −39.8 ‰; *Fig. S3b*), certain alternation of the $\delta^{13}C$ values between consecutive carbons within the alkyl chain characteristic of biogenic hydrocarbons (Georgiou and Deamer, 2014) was still observed (*Fig. S3a*). In addition, the ^{13}C-depleted isotopic signatures observed in general in all the organics in the Ronda springs (Figs. 3 and *S3*) imply that, despite the high pH of the waters, the hydrocarbons wouldn't have been synthesized under CO_2 limitation, since that would have involved less fractionation and thus less negative $\delta^{13}C$ values. Indeed, Etiope et al. (2016) explained the little CO_2 detected in the Ronda springs as derived from the intrusion of more recent carbon sources such as atmospheric CO_2. In such conditions, an abiotic synthesis of the *n*-alkanes seems less likely than a biogenic one. Although an abiogenic origin of the *n*-alkanes in the groundwater samples can't be completely ruled out, their considerably depleted isotopic signatures pointed towards a dominant biogenic origin. In the travertines the biogenicity of *n*-alkanes was even clearer and further supported by the presence at higher concentration of other hydrocarbons of unambiguous biogenic origin (Georgiou and Deamer, 2014) such as branched and unsaturated alkanes (Table 2).

Another qualitative difference between groundwater and travertines was the detection only in the former of a hopanoids series (C_{27} to C_{35}; *Database S1*). Hopanoids are amphiphilic pentacyclic triterpenoids that eubacteria synthesize as essential membrane lipids with rigidifying function (Brocks and Summons, 2003). Depending on their stereochemical configuration (*Fig. S6*), hopanoids can be considered recent or fresh biomarkers (i.e. 17β[H],21β[H] stereochemistry and R configuration at C_{22}), or rather ancient or thermally mature biomarkers (i.e. 17α[H],21β[H] stereochemistry, with R and S configuration at C_{22}) (Seifert and Moldowan, 1980; Peters et al., 2005). The maturity of the C_{31}-C_{35} αβ hopanes can be assessed by using the 22S/(22S + 22R) ratio (*Fig. S6*), showing values lower than 0.5 in relatively fresh biological samples and values from 0.57 to 0.62 in organic matter with a higher degree of maturation, such as that found in petroleum (Seifert and Moldowan, 1980; Peters et al., 2005). In the Ronda groundwater samples, the C_{31}-C_{35} αβ hopanes showed ratios ranging from 0.46 to 0.65 (Fig. 5c), thus reflecting a considerable aging (maturity) of the polycyclic biomarkers.

This maturity could be due to the fact that the hopanes would have originated from beyond the serpentinization environment (allochthonous microbial sources), and their transit through the Ronda peridotites system could have shifted their fresh configuration to a more thermodynamically stable structure by the effect of moderately high temperatures. Based on CH_4 clumped isotopes, the abiotic formation of CH_4 in some of the hyperalkaline springs (i.e. BP) likely occurred at a temperature below 150 °C (Ojeda et al., 2023). Interestingly, Etiope et al. (2016) described in the BP spring a bubbling of CH_4 whose carbon dated from >50,000 years ago, despite the shorter residence time of the spring water (ca. >60 to 2300 years). They proposed that water was a mere carrier of the older CH_4 and likely other hydrocarbons (e.g. *n*-alkanes), which would have been synthesized somewhere else >

50,000 years ago, without knowing exactly when and where (Etiope et al., 2016). We hypothesize that the ancient (i.e. mature) hopanoids detected in our seven groundwater samples may have similarly originated from prokaryotic sources distant in space and/or time and were subsequently transported by deep groundwater through the serpentinized system to the surface. During the transit towards the surface the scarce hopanoids would have mixed up with more abundant organics from diverse autochthonous sources (particularly phototrophs), hence resulting underrepresented in the travertine biomarkers record.

Thus, the travertine deposits represent temporal and spatial reservoirs of biomarkers from the different life forms inhabiting the serpentinization environment and influenced areas, acting as paleoenvironmental archives of present-and-past, subsurface-and-surface, and autochthonous-and-allochthonous biomarkers. When groundwater bearing more or less altered organics from autochthonous (serpentinization system) and allochthonous (somewhere else in the subsurface) biogenic sources ascend and encounters surface water from rainfall, runoff, rivers or streams, mixes and incorporates additional inputs of fresher organic matter from autochthonous (epiperidotitic springs) and allochthonous (meteoric water) sources developed at the surface. Surface precipitation of carbonates upon the interaction of Ca-OH groundwater with Mg-HCO_3 surface and subsurface waters favors the trapping of biomarkers of diverse origin. On the one hand, the travertine deposits encode information about life developed at the surface (dominantly phototrophs) and subsurface (chemolithotrophs, methanogens/methanotrophs), including those from the serpentinized system (autochthonous) and distal scenarios connected with it (allochthonous). On the other hand, they receive biomass from surface runoff and surrounding vegetation that accumulates over time, preserving data of present and past life harbored by or around the serpentinized system. Consequently, the poor biomarker profile in groundwater (i.e. few and scarce biomarkers) becomes more varied and concentrated in the associated deposits by i) mixing with additional biosources at the surface and ii) concentrating over time the few traces of subsurface life, thus acting as amplifiers of the deep life signal.

These results are relevant to the search for life on Mars, where there may be no active serpentinization at present but there was in the Noachian, and a possible life hosted by this alteration process could have left traces in associated deposits. Serpentine outcrops have been reported at different Noachian terrains (e.g. Claritas Rise, Nili Fossae, Isidis basin, and several locations on the southern highlands), suggesting that active serpentinization was a common and widespread process on early Mars (Quesnel et al., 2009; Liu et al., 2022; Ehlmann et al., 2010). If these Martian regions are determined to have hosted ancient serpentinization processes involving energy release and production of H_2, which is a suitable energy source for chemosynthetic microbial life, they represent a promising target for the search for its putative fossil biomarkers. In addition, Martian paleolakes with likely high carbonate alkalinity due to high pCO_2 and near-ambient temperature conditions in the ancient surface of Mars (i.e. thicker atmosphere) could have been an alternative or complementary source of carbonate deposits on Mars (Hurowitz et al., 2023), with capacity to concentrate phosphate and cyanide that are critical for molecular synthesis in the origin of life (Toner and Catling, 2019). This may be the case in the Jezero crater, where carbonate-rich strata are concentrated in marginal deposits between the crater rim and the delta (Horgan et al., 2020). Whether the result of serpentinization processes or evaporation in high-alkalinity palaeolakes, the scarce carbonate deposits on Mars are proving to be a key target for searching for traces of a possible Martian life. The argument for considering Martian serpentinization-associated carbonates a strategic target for life detection is twofold. One, they provide indirect access to the deep subsurface, which may harbor or have harbored an active microbial (likely chemolithotrophic) ecosystem, whose biomarkers could have been carried by serpentinization-driven springs towards the surface becoming trapped in travertine deposits after precipitation. Second, carbonate deposits are good matrices proven to provide long-term preservation of biosignatures (e.g. Onstott et al., 2019; Pierce and Brazelton, 2023; Sánchez-García et al., 2021). Given the relatively long lifetime of lipid biomarkers, their analysis holds promise as tool for investigating molecular or isotopic fingerprints of a possible microbial life in ancient serpentinization environments (or paleolakes with high carbonate alkalinity) on the neighbor planet. Investigations of such geostable biomarkers at serpentinite-hosted ecosystems or lacustrine analogues on Earth will be instrumental in informing sample collection and analysis strategies for the international Mars Sample Return mission on Jezero Crater.

4. Conclusions

Serpentinization provides propitious conditions for the emergence and development of life in the active subsurface of a planet. Exploring serpentinization-hosted ecosystems on Earth allows reconstructing the carbon cycle in environments of such relevance for early life and helps identify putative biosignatures in analogous serpentinizing systems on Mars. Here, we investigated the occurrence of subsurface life associated with active serpentinization in one of the largest outcrops of subcontinental mantle peridotite in the world (Ronda). Based on the molecular and compound-specific isotopic analysis of organics, we identified biogenic fingerprints in groundwater and associated travertines of seven hyperalkaline springs, with qualitative and quantitative differences between the two types of samples. Organics were consistently less concentrated in the groundwater samples. Their molecular profiles represented an admixture of abiotic and biogenic sources, the latter contributing with ancient and mature hopanes and *n*-alkanes (most likely allochthonous), as well as modern and mostly prokaryotic biomarkers (most likely autochthonous). In contrast, the travertine deposits recorded more abundant and varied biomarkers, both prokaryotic and eukaryotic, autochthonous and allochthonous. The deposits accumulate subsurface and surficial inputs over time, thus representing spatial and temporal archives of biomarkers from serpentinization-related life. The detection of molecular and isotopic fingerprints of methanogenic/methanotrophic activity in two of the Ronda hyperalkaline springs (FA and BFA) illustrates the occurrence of such metabolism in serpentinite-hosted environments and raises the hopes of finding comparable biomarkers in ancient serpentinization scenarios on Mars. Reconstructing the biological activity and metabolic interactions in serpentinization environments by decoding the biomarkers profile in associated deposits on the surface offers an interesting avenue to indirectly explore the presence of life of dislocated time (past) and/or space (allochthonous). This is crucial for the search of life on Mars, where the time most likely to have harbored life (if any) has already passed.

CRediT authorship contribution statement

Laura Sánchez-García: Conceptualization, Investigation, Supervision, Writing – original draft, Writing – review & editing. **Daniel Carrizo:** Conceptualization, Data curation, Formal analysis, Investigation, Methodology, Visualization, Writing – review & editing. **Pablo Jiménez-Gavilán:** Investigation, Validation, Visualization, Writing – review & editing. **Lucía Ojeda:** Investigation, Validation, Visualization, Writing – review & editing. **Víctor Parro:** Visualization, Writing – review & editing. **Iñaki Vadillo:** Investigation, Supervision, Validation, Writing – review & editing.

Uncited references

Declaration of competing interest

The authors declare that they have no known competing financial interests or personal relationships that could have appeared to influence the work reported in this paper.

Data availability

Data will be made available on request.

Acknowledgments

This work was funded by MCIN/AEI/10.13039/501100011033 and "ESF Investing in your future" through the grants RYC2018-023943-I (L.S.-G.) and projects ESP2017-87690-C3-3-R (D.C.) and PID2021-126746NB-I00 (V.P. and L.S.-G.). This article is a contribution to the Project "Hydrogeochemistry of the Ronda Peridotites: Characterization of the groundwater and associated methane - UMA18-FEDERJA-101" funded by the European Regional Development Fund (FEDER) and Junta de Andalucía and the UMA project "Isotopic characterization of methane sources in the province of Málaga". It is also a contribution to the Research Group RNM-308 (Group of Hydrogeology) and RNM-128 of the Junta de Andalucía.

Appendix A. Supplementary data

Supplementary data to this article can be found online at https://doi.org/10.1016/j.scitotenv.2023.169045.

References

Acosta-Vigil, A., Rubatto, D., Bartoli, O., Cesarec, B., Melid, S., Pedrera, A., Azor, A., Tajčmanová, L., 2014. Age of anatexis in the crustal footwall of the Ronda peridotites, S Spain. Lithos 210–211, 147–167.

Batsale, M., et al., 2021. Biosynthesis and functions of very-long-chain fatty acids in the responses of plants to abiotic and biotic stresses. Cells 10 (6), 1284.

Berg, I.A., et al., 2010. Autotrophic carbon fixation in archaea. Nat. Rev. Microbiol. 8, 447–460.

Birgel, D., Himmler, T., 2008. A new constraint on the antiquity of anaerobic oxidation of methane: late Pennsylvanian seep limestones from southern Namibia. Geology 36, 543–546.

Bowman, J.P., Skerratt, J.H., Nichols, P.D., Sly, L.I., 1991. Phospholipid fatty acid and lipopolysaccharide fatty acid signature lipids in methane-utilizing bacteria. FEMS Microbiol. Lett. 85, 15–22.

Bradley, A.S., Fredricks, H., Hinrichs, K.U., Summons, R.E., 2009. Structural diversity of diether lipids in carbonate chimneys at the Lost City Hydrothermal Field. Org. Geochem. 40, 1169–1178.

Brazelton, W.J., et al., 2010. Archaea and bacteria with surprising microdiversity show shifts in dominance over 1,000-year time scales in hydrothermal chimneys. Proc. Natl. Acad. Sci. U. S. A. 107, 1612–1617.

Brazelton, W.J., Nelson, B., Schrenk, M.O., 2012. Metagenomic evidence for H_2 oxidation and H_2 production by serpentinite-hosted subsurface microbial communities. Front. Microbiol. 2, 1–16.

Brocks, J.J., Schaeffer, P., 2008. Okenane, a biomarker for purple sulfur bacteria (Chromatiaceae), and other new carotenoid derivatives from the 1640 Ma Barney Creek Formation. Geochim. Cosmochim. Acta 72, 1396–1414.

Brocks, J.J., Summons, R.E., 2003. Sedimentary hydrocarbons, biomarkers for early life. In: Treatise on Geochemistry, 8–9, pp. 63–115.

Carrizo, D., Sánchez-García, L., Rodriguez, N., Gómez, F., 2019. Lipid biomarker and carbon stable isotope survey on the Dallol hydrothermal system in Ethiopia. Astrobiology 19, 1474–1489.

Coates, R.C., et al., 2014. Characterization of cyanobacterial hydrocarbon composition and distribution of biosynthetic pathways. PLoS One 9, e85140.

Cody, G.D., Scott, J.H., 2007. The roots of metabolism. In: Sullivan, I.I.I.W.T., Baross, J. (Eds.), Planets and Life: The Emerging Science of Astrobiology. UK Cambridge University Press, Cambridge, pp. 174–186.

Didyk, B.M., Simoneit, B.R.T., Brassell, S.C., Eglinton, G., 1978. Organic geochemical indicators of palaeoenvironmental conditions of sedimentation. Nature 272, 216–222.

Dijkman, N.A., Boschker, H.T.S., Stal, L.J., Kromkamp, J.C., 2010. Composition and heterogeneity of the microbial community in a coastal microbial mat as revealed by the analysis of pigments and phospholipid-derived fatty acids. J. Sea Res. 63, 62–70.

Ehlmann, B.L., Mustard, J.F., Murchie, S.L., 2010. Geologic setting of serpentine deposits on Mars. Geophys. Res. Lett. 37, L06201. https://doi.org/10.1029/2010GL042596.

Ehlmann, B.L., et al., 2011. Subsurface water and clay mineral formation during the early history of Mars. Nature 479, 53–60.

Elvert, M., Suess, E., Whiticar, M.J., 1999. Anaerobic methane oxidation associated with marine gas hydrates: superlight C-isotopes from saturated and unsaturated C_{20} and C_{25} irregular isoprenoids. Naturwissenschaften 86, 295–300.

Etiope, G., et al., 2016. Abiotic methane seepage in the Ronda peridotite massif, southern Spain. Appl. Geochem. 66, 101–113.

Georgiou, C.D., Deamer, D.W., 2014. Lipids as universal biomarkers of extraterrestrial life. Astrobiology 14, 541–549.

Gervilla, F., Gutiérrez-Narbona, R., Fenoll Hach-Alí, P., 2002. The origin of different types of magmatic mineralizations from small-volume melts in the lherzolite massifs from the Serranía de Ronda (Málaga, Spain). Boletín de la Sociedad Española de Mineralogía 25, 79–96.

Giampouras, M., et al., 2019. Geochemistry and mineralogy of serpentinization-driven hyperalkaline springs in the Ronda peridotites. Lithos 350–351 (2019), 105215.

Goad, L.J., Akihisa, T., 1997. Analysis of Sterols. Blackie Academic & Professional, London.

Goosens, H., De Leeuw, J.W., Schenck, P.A., Brassell, S.C., 1984. Tocopherols as likely precursors of pristane in ancient sediments and crude oils. Nature 312, 440–442.

Grimalt, J.O., de Wit, R., Teixidor, P., Albaigés, J., 1992. Lipid biogeochemistry of Phormidium and Microcoleus mats. Org. Geochem. 19, 509–530.

Hayes, J.M., 2001. Fractionation of carbon and hydrogen isotopes in biosynthetic processes. Rev. Mineral. Geochem. 43 (1), 225–277.

Hays, L.E., et al., 2017. Biosignature preservation and detection in Mars analog environments. Astrobiology 17, 363–400.

Hedges, J.I., Prahl, F.G., 1993. Early diagenesis: consequences for applications of molecular biomarkers. In: Engel, M.H., Macko, S.A. (Eds.), Organic Geochemistry. Topics in Geobiology. Springer, pp. 237–253.

Hinrichs, K.U., Summons, R.E., Orphan, V., Sylva, S.P., Hayes, J.M., 2000. Molecular and isotopic analysis of anaerobic methaneoxidizing communities in marine sediments. Org. Geochem. 31, 1685–1701.

Holm, N.G., Dumont, M., Ivarsson, M., Konn, C., 2006. Alkaline Fluid Circulation in Ultramafic Rocks and Formation of Nucleotide Constituents: A Hypothesis. Geochem, Trans, p. 7.

Horgan, B.H.N., Anderson, R.B., Dromart, G., Amador, E.S., Rice, M.S., 2020. The Mineral Diversity of Jezero Crater: Evidence for Possible Lacustrine Carbonates on Mars. Elsevier Inc.

House, C.H., Schopf, J.W., Stetter, K.O., 2003. Carbon isotopic fractionation by Archaeans and other thermophilic prokaryotes. Org. Geochem. 34, 345–356.

House, C.H., Beal, E.J., Orphan, V.J., 2011. The apparent involvement of ANMEs in mineral dependent methane oxidation, as an analog for possible martian methanotrophy. Life 1, 19–33.

House, C.H., et al., 2022. Depleted carbon isotope compositions observed at Gale crater. Mars. Proc. Natl. Acad. Sci. 119, e2115651119.

Hügler, M., Sievert, S.M., 2011. Beyond the Calvin cycle: autotrophic carbon fixation in the ocean. Annu. Rev. Mar. Sci. 3, 261–289.

Hurowitz, J.A., Catling, D.C., Fischer, W.W., 2023. High Carbonate Alkalinity Lakes on Mars and Their Potential Role in an Origin of Life Beyond Earth. Elements, 19. pp. 37–44. (2023).

Jiménez-Gavilán, P., Vadillo Pérez, I., Scapini Gallardo, R., 2021. Caracterización hidrogeoquímica e isotópica preliminar de los manantiales epiperidotíticos de las Peridotitas de Ronda. Geotemas 18, 303–307. ISSN 1576-5172. https://sociedadgeologica.org/publicaciones/geotemas/geo-temas-18/.

Kaneda, T., 1991. Iso- and anteiso-fatty acids in bacteria: biosynthesis, function, and taxonomic significance. Microbiol. Rev. 55, 288–302.

Kates, M., 1993. Membrane lipids of Archaea. In: Kates, M., Kushner, D.J., Matheson, A.T. (Eds.), The Biochemistry of Archaea (Archaebacteria). Elsevier, Amsterdam, pp. 261–295.

Klein, F., et al., 2015. Fluid mixing and the deep biosphere of a fossil Lost City-type hydrothermal system at the Iberia Margin. Proc. Natl. Acad. Sci. U. S. A. 112, 12036–12041.

Liu, Y., et al., 2022. An olivine cumulate outcrop on the floor of Jezero crater, Mars. Science 377, 1513–1519.

Martin, W., Baross, J., Kelley, D., Russell, M.J., 2008. Hydrothermal vents and the origin of life. Nat. Rev. Microbiol. 6, 805–814.

McCollom, T.M., Seewald, J.S., 2007. Abiotic synthesis of organic compounds in deep-sea hydrothermal environments. Chem. Rev. 107, 382–401.

Milliken, R.E., Rivkin, A.S., 2009. Brucite and carbonate assemblages from altered olivine-rich materials on Ceres. Nat. Geosci. 2, 258–261.

Mottl, M.J., Komor, S.C., Fryer, P., Moyer, C.L., 2003. Deep-slab fluids fuel extremophilic Archaea on a Mariana forearc serpentinite mud volcano: ocean drilling program leg 195. Geochem. Geophys. Geosyst. 4, 1–14.

Muyzer, G., Stams, A.J.M., 2008. The ecology and biotechnology of sulphate-reducing bacteria. Nat. Rev. Microbiol. 6, 441–454.

Nealson, K.H., Inagaki, F., Takai, K., 2005. Hydrogen-driven subsurface lithoautotrophic microbial ecosystems (SLiMEs): do they exist and why should we care? Trends Microbiol. 13, 405–410.

Newman, S.A., et al., 2020. Lipid biomarker record of the serpentinite-hosted ecosystem of the Samail ophiolite, Oman and implications for the search for biosignatures on Mars. Astrobiology 20, 830–845.

Obata, M., 1980. The Ronda peridotite: garnet-, spinel-, and plagioclase-lherzolite facies and the PeT trajectories of high temperature mantle emplacement. J. Petrol. 21, 533e572.

Ojeda, L., Etiope, G., Jiménez-Gavilán, P., Martonos, I.M., Röckmann, T., Popa, M.E., Sivan, M., Castro-Gámez, A.F1., Benavente, J., Vadillo, I., 2023. Combining methane clumped and bulk isotopes, temporal variations in molecular and isotopic

composition, and hydrochemical and geological proxies to understand methane's origin in the Ronda peridotite massifs (Spain). Chem. Geol. 121799. https://doi.org/10.1016/j.chemgeo.2023.121799.
Onstott, T.C., Ehlmann, B.L., Sapers, H., et al., 2019. Paleo-rock-hosted life on earth and the search on Mars: a review and strategy for exploration. Astrobiology 19, 1230–1262. https://doi.org/10.1089/ast.2018.1960.
Peters, K.E., Walters, C.C., Moldowan, J.M., 2005. The Biomarker Guide - Part II - Biomarkers and Isotopes in Petroleum Exploration and Earth History. Cambridge University Press, New York.
Pierce, M.P., Brazelton, W.J., 2023. Genetic biosignatures of deep-subsurface organisms preserved in carbonates over a 100,000 year timescale at a surface-accessible Mars analog site in southeastern Utah. Astrobiology 23. https://doi.org/10.1089/ast.2022.0139.
Preuß, A., Schauder, R., Fuchs, G., Stichler, W., 1989. Carbon isotope fractionation by autotrophic bacteria with three different CO_2 fixation pathways. Zeitschrift fur Naturforsch. - Sect. C J. Biosci. 44, 397–402.
Proskurowski, G., et al., 2008. Abiogenic hydrocarbon production at lost city hydrothermal field. Science 319, 604–607.
Quesnel, Y., et al., 2009. Serpentinization of the martian crust during Noachian. Earth Planet. Sci. Lett. 277, 184–193.
Rohmer, M., Bouvier-Nave, P., Ourisson, G., 1984. Distribution of hopanoid triterpenes in prokaryotes. J. Gen. Microbiol. 130, 1137–1150.
Rushdi, A.I., Simoneit, B.R.T., 2001. Lipid formation by aqueous Fischer-Tropsch-type synthesis over a temperature range of 100 to 400 °C. Orig. Life Evol. Biosph. 31, 103–118.
Russell, M., Grimalt, J.O., Hartgers, W.A., Taberner, C., Rouchy, J.M., 1997. Bacterial and algal markers in sedimentary organic matter deposited under natural sulphurization conditions (Lorca Basin, Murcia, Spain). Org. Geochem. 26, 605–625.
Russell, M.J., Hall, A.J., Martin, W., 2010. Serpentinization as a source of energy at the origin of life. Geobiology 8, 355–371.
Saito, R., et al., 2017. Tentative identification of diagenetic products of cyclic biphytanes in sedimentary rocks from the uppermost Permian and Lower Triassic. Org. Geochem. 111, 144–153.
Sánchez-García, L., et al., 2021. Time-integrative multibiomarker detection in Triassic–Jurassic rocks from the Atacama Desert: relevance to the search for basic life beyond Earth. Astrobiology 21, 1421–1437.
Schidlowski, M., 2001. Carbon isotopes as biogeochemical recorders of life over 3.8 Ga of earth history: evolution of a concept. Precambrian Res. 106, 117–134.
Schrenk, M.O., Brazelton, W.J., Lang, S.Q., 2013. Serpentinization, carbon, and deep life. Rev. Mineral. Geochem. 75, 575–606.
Schulte, M., Blake, D., Hoehler, T., McCollom, T., 2006. Serpentinization and its implications for life on the early Earth and Mars. Astrobiology 6, 364–376.
Seifert, W.K., Moldowan, J.M., 1980. The effect of thermal stress on source-rock quality as measured by hopane stereochemistry. Phys. Chem. Earth 12, 229–237.
Sephton, M.A., 2014. In: Falkowski, P.G., Freeman, K.H. (Eds.), Treatise on Geochemistry. 2nd edition. https://doi.org/10.1016/B978-0-08-095975-7.01002-0.
Shiea, J., Brassell, S.C., Ward, D.M., 1990. Mid-chain branched mono- and dimethyl alkanes in hot spring cyanobacterial mats: a direct biogenic source for branched alkanes in ancient sediments? Org. Geochem. 15, 223–231.
Sinninghe Damsté, J.S., Rijpstra, W.I.C., Schouten, S., Fuerst, J.A., Jetten, M.S.M., Strous, M., 2007. The occurrence of hopanoids in planctomycetes: implications for the sedimentary biomarker record. Org. Geochem. 35, 561–566.
Skennerton, C.T., Chourey, K., Iyer, R., et al., 2017. Methane-fueled syntrophy through extracellular electron transfer: uncovering the genomic traits conserved within diverse bacterial partners of anaerobic methanotrophic archaea. mBio 8, e00530-17. https://doi.org/10.1128/mBio.00530-17.
Sorokin, D.Y., Tourova, T.P., Mußmann, M., Muyzer, G., 2008. Dethiobacter alkaliphilus gen. nov. sp. nov., and Desulfurivibrio alkaliphilus gen. nov. sp. nov.: two novel representatives of reductive sulfur cycle from soda lakes. Extremophiles 12, 431–439.
Summons, R.E., Welander, P.W., Gold, D.A., 2021. Lipid biomarkers: molecular tools for understanding ancient microbial life. Nat. Rev. Microbiol. 63–65.
Suzuki, S., et al., 2013. Microbial diversity in the Cedars, an ultrabasic, ultrareducing, and low salinity serpentinizing ecosystem. Proc. Natl. Acad. Sci. U. S. A. 110, 15336–15341.
Tiago, I., Veríssimo, A., 2013. Microbial and functional diversity of a subterrestrial high pH groundwater associated to serpentinization. Environ. Microbiol. 15, 1687–1706.
Toner, J. D., Catling, D. C., Alkaline lake settings for concentrated prebiotic cyanide and the origin of life. Geochim. Cosmochim. Acta 260, 124–132.
Vadillo, I., Urresti, B., Jiménez-Gavilán, P., Martos-Rosillo, S., Durán, J.J., Benavente, J., Carrasco, F., Pedrera, A., 2015. Preliminary hydrochemical characterization of Ronda peridotite massif (Málaga province). In: El Agua en Andalucía: El Agua, Clave Medioambiental y Socioeconómica. pp. 515–525.
Van Der Meer, M.T.J., Schouten, S., De Leeuw, J.W., Ward, D.M., 2000. Autotrophy of green non-sulphur bacteria in hot spring microbial mats: biological explanations for isotopically heavy organic carbon in the geological record. Environ. Microbiol. 2, 428–435.
Vance, S., et al., 2007. Hydrothermal systems in small ocean planets. Astrobiology 7, 987–1005.
Vinnichenko, G., Jarrett, A.J.M., Hope, J.M., Brocks, J.J., 2020. Discovery of the oldest known biomarkers provides evidence for phototrophic bacteria in the 1.73 Ga Wollogorang Formation, Australia. Geobiology 18, 544–559.
Volkman, J.K., 1986. A review of sterol markers for marine and terrigenous organic matter. Org. Geochem. 9, 83–99.
Webster, C.R., et al., 2013. Isotope ratios of H, C, and O in CO_2 and H_2O of the martian atmosphere. Science 341, 260–263.
Whiticar, M.J., 1999. Carbon and hydrogen isotope systematics of bacterial formation and oxidation of methane. Chem. Geol. 161, 291–314.
Yu, S., Ni, D., 2023. Serpentinisation is required for the magnetisation of the Martian crust. Res. Astron. Astrophys. 0–14.